The Astrophysical Journal Letters, 882:L15 (7pp), 2019 September 10 https://doi.org/10.3847/2041-8213/ab3d44

SN 2018hna: 1987A-like Supernova with a Signature of Shock Breakout

Avinash Singh[1,2], D. K. Sahu[1], G. C. Anupama[1], Brajesh Kumar[1], Harsh Kumar[3,15], Masayuki Yamanaka[4,5], Petr V. Baklanov[6,7], Nozomu Tominaga[8,9], Sergei I. Blinnikov[7,9,10], Keiichi Maeda[11], Anirban Dutta[1], Varun Bhalerao[3], Ramya M. Anche[1], Sudhanshu Barway[1], Hiroshi Akitaya[5], Tatsuya Nakaoka[12], Miho Kawabata[11,12], Koji S Kawabata[5], Mahito Sasada[5], Kengo Takagi[12], Hiroyuki Maehara[13], Keisuke Isogai[4], Masaru Kino[4], Kenta Taguchi[11], and Takashi Nagao[14]
[1] Indian Institute of Astrophysics, Koramangala 2nd Block, Bengaluru 560034, India; avinash21292@gmail.com, avinash.singh@iiap.res.in
[2] Joint Astronomy Programme, Department of Physics, Indian Institute of Science, Bengaluru 560012, India
[3] Physics Department, Indian Institute of Technology Bombay, Powai, Mumbai 400076, India
[4] Okayama Observatory, Kyoto University, 3037-5 Honjo, Kamogata-cho, Asakuchi, Okayama 719-0232, Japan
[5] Hiroshima Astrophysical Science Center, Hiroshima University, Higashi-Hiroshima, Hiroshima 739-8526, Japan
[6] National Research Nuclear University MEPhI, Kashirskoe sh. 31, Moscow 115409, Russia
[7] National Research Center "Kurchatov institute," Institute for Theoretical and Experimental Physics (ITEP), 117218 Moscow, Russia
[8] Department of Physics, Faculty of Science and Engineering, Konan University, 8-9-1 Okamoto, Kobe, Hyogo 658-8501, Japan
[9] Kavli Institute for the Physics and Mathematics of the Universe (WPI), The University of Tokyo Institutes for Advanced Study, The University of Tokyo, 5-1-5 Kashiwanoha, Kashiwa, Chiba 277-8583, Japan
[10] Sternberg Astronomical Institute, M.V. Lomonosov Moscow State University, Universitetski pr. 13, 119234 Moscow, Russia
[11] Department of Astronomy, Kyoto University, Kitashirakawa-Oiwake-cho, Sakyo-ku, Kyoto 606-8502, Japan
[12] Department of Physical Science, Hiroshima University, Kagamiyama 1-3-1, Higashi-Hiroshima 739-8526, Japan
[13] Okayama Branch Office, Subaru Telescope, National Astronomical Observatory of Japan, NINS, Kamogata, Asakuchi, Okayama 719-0232, Japan
[14] European Southern Observatory, Karl-Schwarzschild-Str. 2, D-85748 Garching b. München, Germany
Received 2019 August 3; revised 2019 August 20; accepted 2019 August 20; published 2019 September 5

Abstract

High-cadence ultraviolet, optical, and near-infrared photometric and low-resolution spectroscopic observations of the peculiar Type II supernova (SN) 2018hna are presented. The early-phase multiband light curves (LCs) exhibit the adiabatic cooling envelope emission following the shock breakout up to ~ 14 days from the explosion. SN 2018hna has a rise time of ~ 88 days in the V band, similar to SN 1987A. A ^{56}Ni mass of $\sim 0.087 \pm 0.004\,M_{\odot}$ is inferred for SN 2018hna from its bolometric LC. Hydrodynamical modeling of the cooling phase suggests a progenitor with a radius $\sim 50\,R_{\odot}$, a mass of $\sim$14–20 $M_{\odot}$, and an explosion energy of ~ 1.7–2.9×10^{51} erg. The smaller inferred radius of the progenitor than a standard red supergiant is indicative of a blue supergiant progenitor of SN 2018hna. A subsolar metallicity ($\sim 0.3\,Z_{\odot}$) is inferred for the host galaxy UGC 07534, concurrent with the low-metallicity environments of 1987A-like events.

Unified Astronomy Thesaurus concepts: Supernovae (1668); Core-collapse supernovae (304); Type II supernovae (1731)

Supporting material: data behind figures

1. Introduction

Core-collapse supernovae (CCSNe) result from the gravitational collapse of stars with a zero-age main sequence (ZAMS) mass $\gtrsim 8\,M_{\odot}$ (Heger et al. 2003). SNe II result from stars that retain their hydrogen envelope at the time of explosion. Theoretical (Grassberg et al. 1971) and observational (Smartt 2009) studies of SNe II indicate a red supergiant (RSG) progenitor. However, the nearest naked-eye supernova in the last four centuries, SN 1987A, showed that a blue supergiant (BSG) can also be a progenitor of SNe II. The presence of a slow rise to the maximum ($\sim$85–100 days) is the distinguishing feature in the light curves (LCs) of SNe II resulting from a BSG (Kleiser et al. 2011). However, extended RSGs can also result in a slow-rising SN II if they synthesize a substantial amount of ^{56}Ni ($\sim 0.2\,M_{\odot}$) in the explosion (e.g., SN 2004ek; Taddia et al. 2016). Theoretical models have shown that fast rotation, low metallicity, and/or interaction in a binary system can indeed lead to the explosion of BSGs as SNe (Podsiadlowski 1992).

In the vast expanse of data on SNe II, only a handful of SNe have shown similarities to SN 1987A (Hamuy & Suntzeff 1990; Pun et al. 1995). These are SN 1998A (Pastorello et al. 2005), SN 2000cb (Utrobin & Chugai 2011), and SN 2005ci (Kleiser et al. 2011), SN 2006V and SN 2006au (Taddia et al. 2012), SN 2009E (Pastorello et al. 2012), SN 2009mw (Takáts et al. 2016), and SN Refsdal (Kelly et al. 2016; Rodney et al. 2016). These will be referred to as 1987A-like events, whereas Type II events with an RSG progenitor will be referred to as normal SNe II. Analysis of 1987A-like events have shown that these arise from rather compact progenitors (BSG, $R < 100\,R_{\odot}$) with a higher ZAMS mass, higher explosion energies ($>10^{51}$ erg), and higher synthesized ^{56}Ni ($\sim 0.1\,M_{\odot}$) when compared to normal SNe II (Pastorello et al. 2012; Taddia et al. 2016).

The collapse of the core in CCSNe is succeeded by a shock wave resulting from the rebound of the infalling matter on the neutron-degenerate protoneutron star (collapsed core). A fraction of the energy lost during this collapse is transferred via neutrino heating to the outer ejecta. The shock accelerates toward the surface of the star, releasing energy in X-ray and UV (Falk & Arnett 1977) due to its high temperature (10^5–10^6 K; Ensman & Burrows 1992). This short-lived ($\sim$thousands in RSGs) phase is labeled as "shock" breakout

[15] LSSTC DSFP Fellow.

and marks the first electromagnetic signature of an SN explosion.

The cooling emission from the heated envelope as a result of the shock breakout has been seen only in a few SNe II such as SN 1987A (Ensman & Burrows 1992), SNLS-04D2dc (Tominaga et al. 2009), SN 2010aq (Gezari et al. 2010), etc. The signature of a shock breakout is generally more prominent in SNe IIb with extended envelopes, e.g., SN 1993J (Richmond et al. 1994) and SN 2011fu (Kumar et al. 2013). The thermal emission from the heated ejecta peaks in the UV spanning a few hours to a couple of days (Nakar & Sari 2010). The shock breakout may be delayed due to the presence of a circumstellar wind as the shock not only has to escape the outer envelope of the SN ejecta, but also the dense wind surrounding it (Ofek et al. 2013). During the breakout, the energy released scales with the progenitor radius and hence the detection of an early emission helps in directly tracing the progenitor properties.

SN 2018hna was discovered by Koichi Itagaki on 2018 October 23.9 UT (JD 2458414.3) in the galaxy UGC 07534. SN 2018hna lies 31″E and 30″N from the nucleus of the host galaxy. A spectrum obtained by Hiroshima One-shot Wide-field POLarimeter (HOWPol; Kawabata et al. 2008) on 2018 October 24.8 UT displayed a prominent P-Cygni profile of Hα categorizing it as an SN II (TNS # 2933).

The photometric and spectroscopic evolution of SN 2018hna is presented in this Letter and discussed in the context of 1987A-like events.

2. Data Acquisition

Optical photometric (*UBVRI*) and spectroscopic observations of SN 2018hna using the 2 m Himalayan Chandra Telescope (HCT), Indian Astronomical Observatory (IAO), Hanle, India began on 2018 October 31.9 UT (JD 2458423.4). The recently installed robotic 0.7 m GROWTH[16]-India telescope (GIT) at IAO followed up SN 2018hna in the SDSS $g'r'i'$ filters starting 2018 November 15.9 UT. SN 2018hna was also monitored with the 1.5 m Kanata Telescope in the optical and the near-infrared using the HOWPol and the Hiroshima Optical and Near-InfraRed camera (HONIR; Akitaya et al. 2014). A few spectra were also obtained using the Kyoto Okayama Optical Low-dispersion Spectrograph with Optical-Fiber Integral Field Unit (KOOLS-IFU; Matsubayashi et al. 2019) mounted on the 3.8 m Seimei telescope, at the Okayama Observatory. Data reduction was performed using standard reduction procedures described in Singh et al. (2018). The follow-up of SN 2018hna is supplemented by data from the public archives of the Zwicky Transient Facility (ZTF; Bellm et al. 2019) in the *g* and *r* bands, from Lasair (Smith et al. 2019), and *Gaia* (Gaia Collaboration et al. 2018) in the *g* band.

The *Neil Gehrels Swift Observatory* (Gehrels et al. 2004) monitored SN 2018hna with the ultraviolet Optical Telescope (UVOT; Roming et al. 2005) beginning 2018 October 23.6 UT. Data reduction was performed using the UVOT data analysis software in HEASOFT (see Kumar et al. 2018).

3. Photometric Evolution

The ultraviolet, optical, and near-infrared LCs of SN 2018hna are shown in Figure 1. The slow rise to the maximum and the broad peak resemble the peculiar Type II SN 1987A. Due to the immediate follow-up with *Swift*, the early LCs in the optical and the ultraviolet bands show a noticeable decline in brightness during the initial phase, followed by a rise to the maximum. This drop can be explained as a result of the rapid cooling of the photosphere proceeding the shock breakout and was also seen in SN 1987A. Hydrodynamic modeling of the early LC constrained the explosion date to be JD 2458411.3, 3 days prior to discovery (see Section 5.1). The peak in the *V*-band LC of SN 2018hna at ∼87.5 days is adopted as the epoch of maximum. This is similar to SN 1987A (∼86 days). A Galactic reddening of $E(B-V) = 0.009 \pm 0.001$ mag along the direction of SN 2018hna was obtained from the dust-extinction map of Schlafly & Finkbeiner (2011). This is consistent with the absence of interstellar Na I D absorption in the spectra of SN 2018hna. No trace of Na I D absorption is seen at the redshift of the host galaxy, concurrent with the high offset of SN 2018hna from the center of the host. A net reddening of $E(B-V) = 0.009 \pm 0.001$ mag is adopted assuming no host extinction. A distance modulus of $\mu = 30.52 \pm 0.29$ mag (12.82 ± 2.02 Mpc) is estimated for the host galaxy UGC 07534 from the mean of the Hubble flow distances provided in the NASA Extragalactic Database (NED[17]) and the Tully–Fisher relation (Karachentsev et al. 2013).

4. Spectroscopic Evolution

The spectral evolution of SN 2018hna is shown in Figure 2(A). The first spectrum of SN 2018hna obtained at ∼12 days shows strong, broad P-Cygni profiles of the Balmer lines, Fe II features, Ca II NIR triplet, and weak Ba II 4554 Å. He I 5876 Å was identified in the early (∼3 days from explosion) spectrum of SN 1987A. However, the feature around 5740 Å is identified as Na I D instead of He I 5876 Å due to the low color temperature (<8000 K) inferred from the spectral energy distribution (SED).

As the SN evolved toward the maximum, features of Na I D, Fe II, Ca II, Ba II, Sc II, Ti II, and Sr II became more prominent. The line identification in the spectrum of ∼73 days is shown in Figure 2(E). The features of Ba II (i.e., 4554 and 6142 Å), which are characteristic of 1987A-like events (Mazzali & Chugai 1995), are also evident in the spectra (>15 days) of SN 2018hna. The prominent features during the late nebular phase (∼256 days) are labeled in Figure 2(D). Feature marked "A" (∼8360 Å) is unidentified and warrants further investigation.

The P-Cygni profile of Hα in SN 2018hna shows a blueshift in its emission feature during the photospheric phase, which settles onto a constant value of ∼600 km s^{-1} during the transition to the radioactive decay phase (>100 days). The blueshift has been seen in a majority of SNe II (including 1987A-like SNe) and has been explained as arising from the steep density profile of the outer SN ejecta (Anderson et al. 2014).

The absorption troughs of H α, H β, and Na I D features in the spectra of SN 2018hna show a "kink" (flux excess) beginning at ∼37 days (see Figure 3). This feature is strongest in the spectrum of ∼102 days and disappeared by ∼112 days. The presence of Ba II in the troughs of Na I D and Hα can possibly explain this feature, although this line blend should be seen as absorption and not an emission during the photospheric phase. This complex fine-structure was also detected in SN 1987A (Hanuschik et al. 1988; Phillips & Heathcote 1989)

[16] Global Relay of Observatories Watching Transients Happen (http://growth.caltech.edu).

[17] https://ned.ipac.caltech.edu

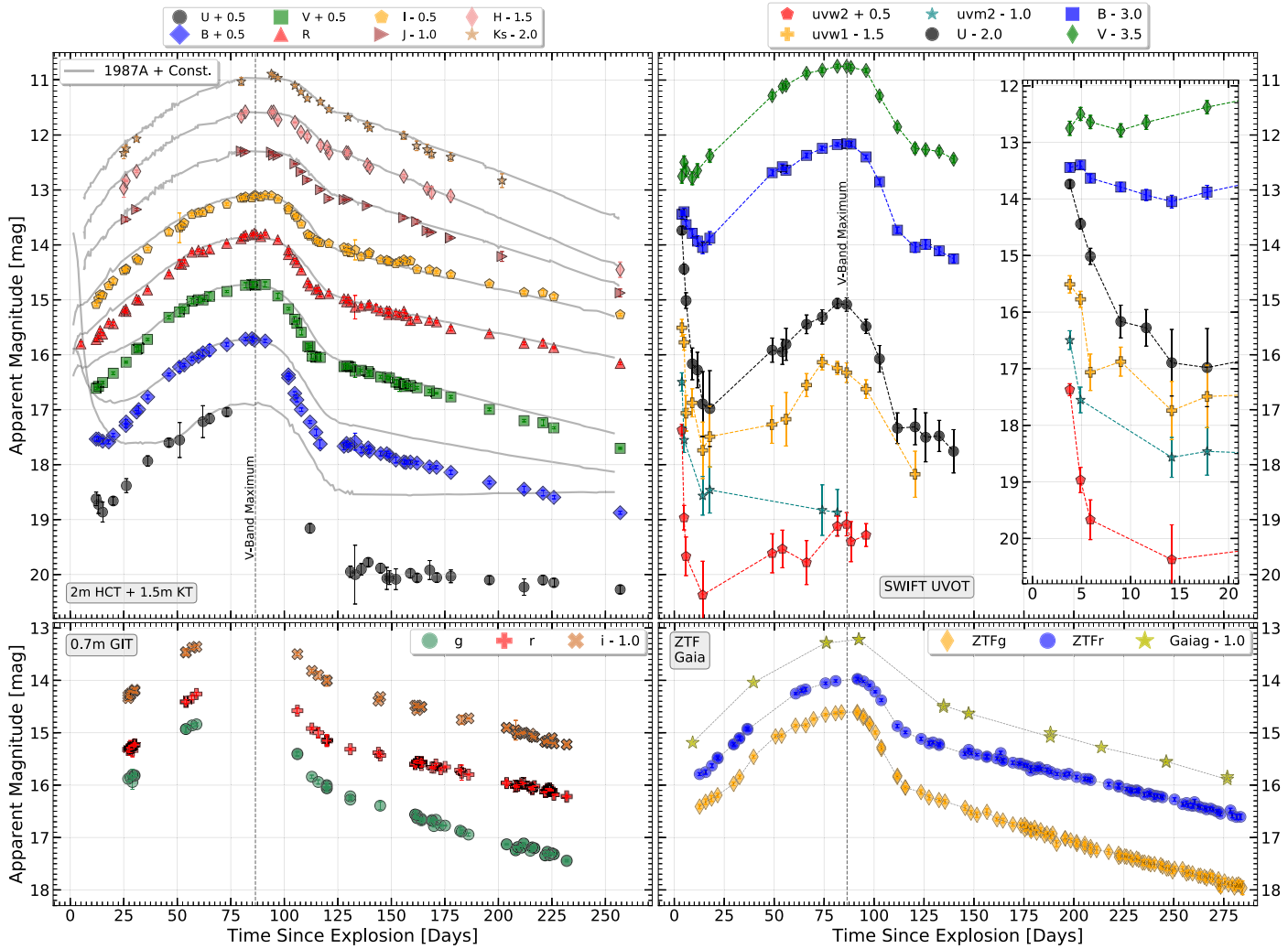

Figure 1. Apparent light curves (LCs) of SN 2018hna. The LCs of SN 1987A were shifted to match the maximum of SN 2018hna. Offsets have been applied for clarity.

(The data used to create this figure are available.)

and comprised a blueshifted flux excess and a redshifted flux deficit, of which only the former is seen in SN 2018hna. The origin of these kinks is likely a result of asymmetry in the line-emitting region. The velocities of these kinks closely follow the photospheric velocity evolution as in SN 1987A and indicate the advent of high-energy radiation from the decay of ^{56}Ni at the photosphere (Phillips & Heathcote 1989).

5. Discussion

SN 2018hna occurred in the outskirts (∼2.5 kpc from the center) of the low-luminosity ($M_B \sim -17.1$ mag) dwarf irregular galaxy (IBm) UGC 07534. The luminosity−metallicity relation of Tremonti et al. (2004) yields an oxygen abundance of 8.14 ± 0.02 for UGC 07534. This indicates a subsolar metallicity (∼0.3 $Z_\odot$) of the host environment of SN 2018hna and is consistent with the occurrence of 1987A-like SNe in late-type galaxies (Sc or later; Pastorello et al. 2012) having subsolar metallicity.

5.1. Cooling Envelope Emission and Explosion Parameters

The early LCs (<14 days) of SN 2018hna distinctly show adiabatic cooling of the shock-heated SN ejecta. The early emission in the *B* and *V* bands shows a rise toward an initial peak. This is a result of the "temperature effect" resulting from the migration of the SN SED into the optical wavelengths while the net bolometric luminosity is still declining (Fremling et al. 2019).

Prominent signature of cooling emission is generally seen in Type II (distinctly in IIb) SNe, arising from an extended envelope surrounding their compact core. A similar emission can be seen for a compact BSG progenitor, e.g., 1987A-like events. Since the cooling emission is generally stronger for a more extended and/or more massive envelope, one could use this emission to infer the properties of the H-rich envelope (Nakar & Sari 2010; Bersten et al. 2012; Nakar & Piro 2014).

The multicolor LCs of an explosion of a BSG star were computed with the multigroup radiation hydrodynamics code STELLA (Blinnikov et al. 2000). The resultant synthetic SED was convolved with the filter transmission function of the respective bandpasses. The multicolor LCs of SN 2018hna during the cooling phase were well reproduced for a star of pre-SN mass $\sim 16\,M_\odot$ (i.e., an ejecta mass $\sim 14\,M_\odot$), a radius of $\sim 50\,R_\odot$, and an explosion energy of $\sim 1.7 \times 10^{51}$ erg (see Figure 4). The explosion epoch was constrained to 3 days prior to the discovery, i.e., JD 2458411.3.

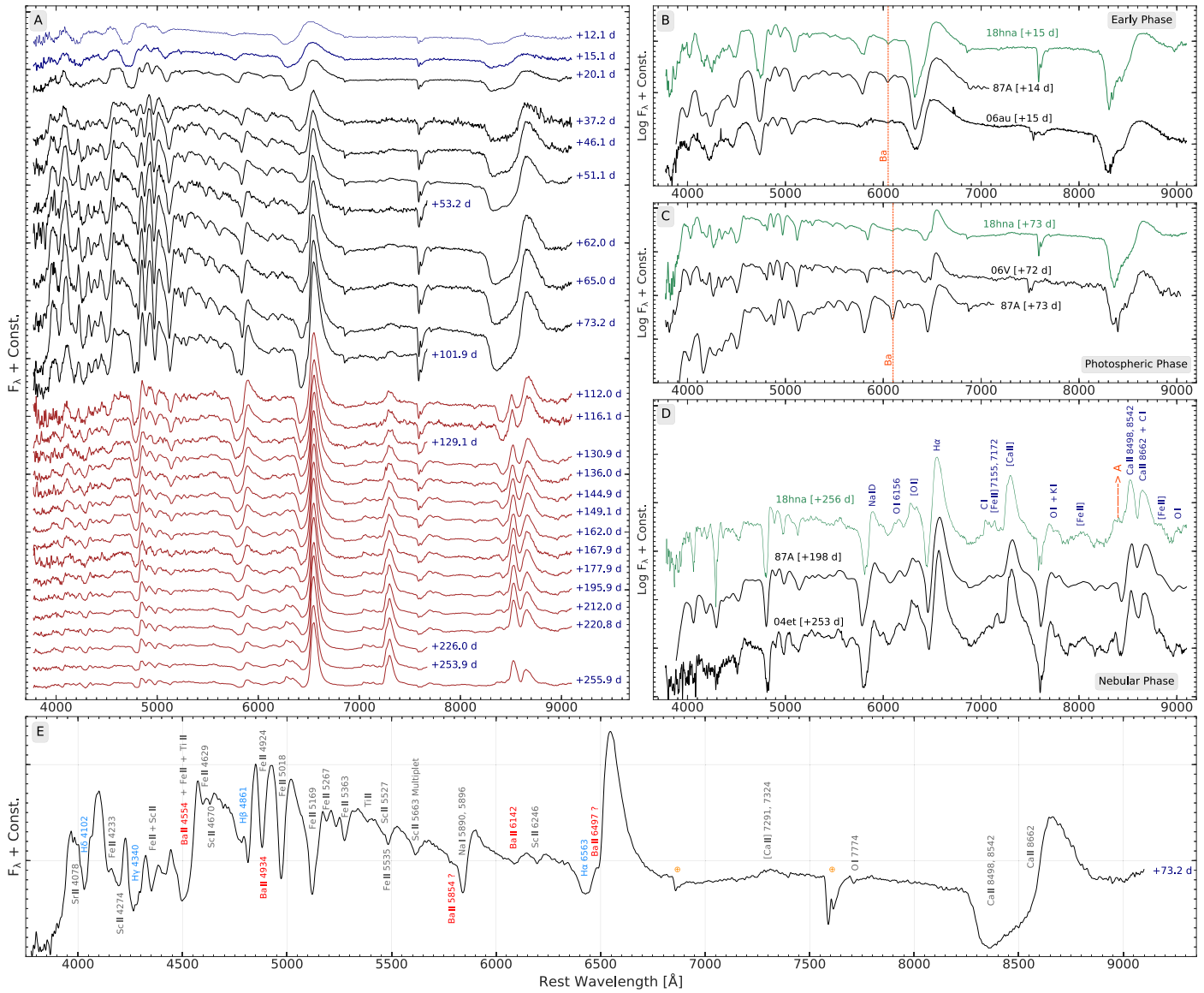

Figure 2. Panel (A): spectroscopic sequence of SN 2018hna. The three different colors depict the cooling envelope (blue), photospheric (black), and nebular (red) phases of the SN. Panels (B)–(D): comparison of SN 2018hna with 1987A-like events. Panel (E): identification of lines in the spectrum of ∼73 days.
(The data used to create this figure are available.)

In the case of a compact progenitor, the drop in temperature after the shock breakout reduces once the temperature reaches the bracket of 6000–8000 K due to the process of recombination. Hence, the luminosity in the redder bands (*VRI*) keeps rising as the temperature falls to this bracket, whereas the luminosity in the UV bands keeps falling as the wavelength evolves to the Wein's part of the spectrum (Nakar & Piro 2014). The inset in Figure 5(A) shows the comparison of SN 2018hna with SN 1987A during the cooling envelope phase. The luminosity and timescale of the cooling emission overlap between the two SNe. This is indicative of similarities in progenitor properties (like radius and the ratio of ejecta energy to mass) between SN 2018hna and SN 1987A. We rule out the delay of the shock breakout due to an immediate circumstellar material, as no observable feature of such an interaction is discernible in the spectral sequence of SN 2018hna.

The long rise time of 1987A-like events can be explained due to the slow diffusion of radiation from the decay of radioactive ^{56}Ni through the massive envelope of the progenitor. Hence, the time taken for the radiation to diffuse through the ejecta is used to estimate the mass using the relation from Arnett (1979) for radioactively powered SNe. Using $E_{87A} = 1.1 \times 10^{51}$ erg s^{-1} and $M_{87A} = 14\,M_{\odot}$ (Blinnikov et al. 2000), diffusion time, $t_d \sim 1.02\,t_d^{1987A}$, and a similar mean opacity, an ejecta mass of ∼19.8 $M_{\odot}$, and an E_{expl} of ∼2.9 × 10^{51} erg are inferred for SN 2018hna.

5.2. Comparison with 1987A-like Events

The Ba II 6142 Å feature in SN 2018hna was identified as early as ∼15 days, similar to SN 1987A, but much earlier in comparison to normal SNe II (seen at ∼50 days). The strength of Ba II features in SN 1987A primarily arises from the overabundance of barium in the entirety of its hydrogen envelope due to the faster cooling of the SN ejecta resulting from its compact progenitor (Mazzali & Chugai 1995). Also,

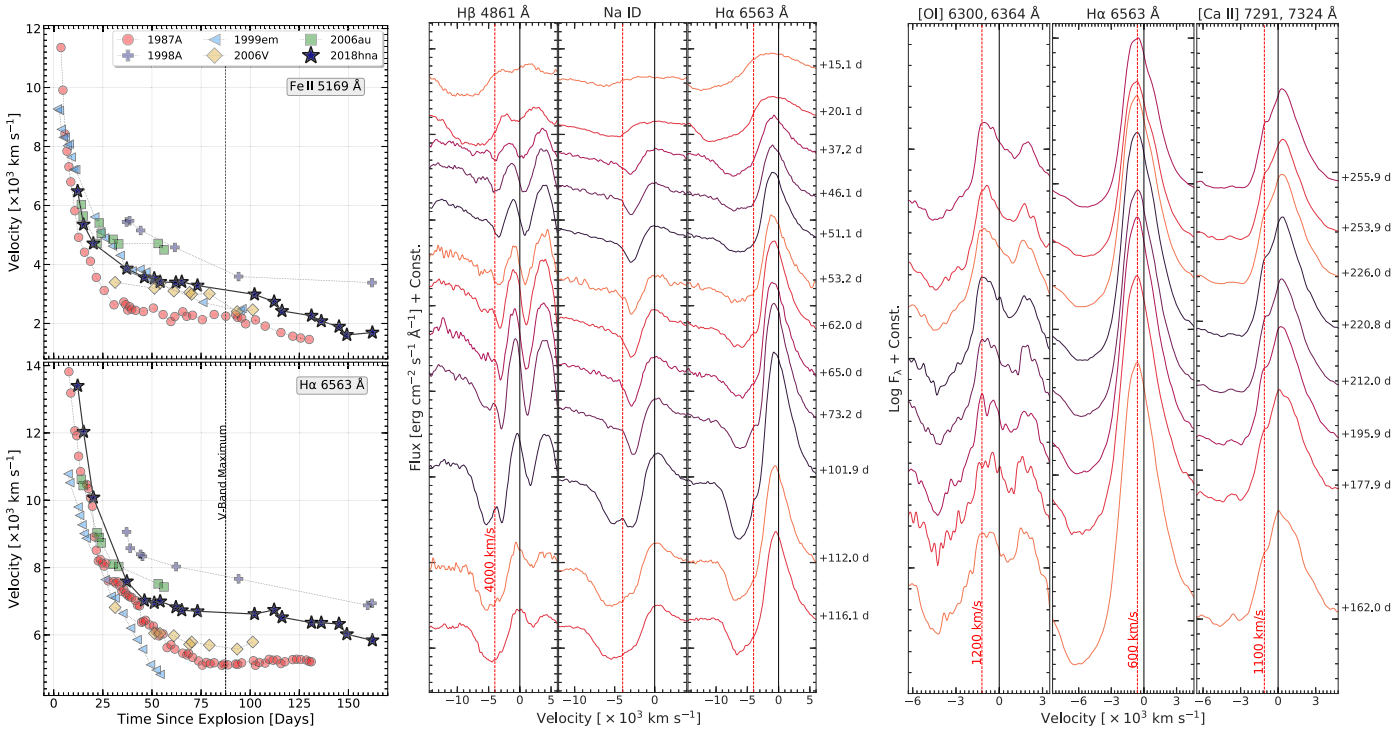

Figure 3. Left panel: line velocity evolution of SN 2018hna. Middle panel: evolution of H β, H α, and Na ID up until ∼120 days. Right panel: evolution of O I, H α, and Ca II during the nebular phase.

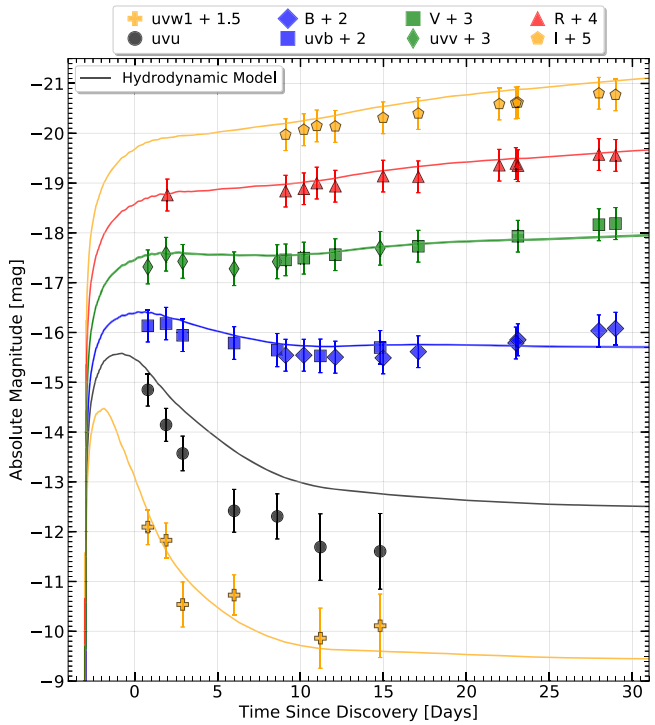

Figure 4. Comparison of early-phase *Swift* LCs with the hydrodynamic model.

slow-expanding ejecta are denser and produce stronger Ba II features in 1987A-like and low-luminosity SNe II (e.g., SN 2005cs; Pastorello et al. 2009). SN 2018hna does not show as strong a Ba II feature as in SN 1987A due to its relatively bluer colors along with a faster photospheric velocity (50% faster at *V*-band maximum). This is evident in the spectral comparison in Figures 2(B)–(D).

The velocity evolution of Hα and the Fe II λ5169 feature of SN 2018hna indicates an evolution similar to SN 1987A during the early phase that subsequently flattens out at a higher velocity (see Figure 3). This is possibly a result of the higher explosion energy in SN 2018hna, which leads to broader line profiles throughout its evolution.

The cooling envelope phase in 1987A-like events shows a steep rise in colors as seen in the evolution of *U*–*V* and *B*–*V* colors (Figures 5(B) and (C)). After the cooling phase, the evolution is almost flat. SN 2018hna, SN 2006au, and SN 2006V are bluer compared to SN 1987A. This agrees with the fact that 1987A-like events with bluer colors tend to be brighter at maximum (Taddia et al. 2016). SN 2018hna is bluer in *U*–*V* by ∼1.6 mag and in *B*–*V* by ∼0.4 mag. Differences in color can partially be attributed to higher line-blanketing in SN 1987A (see Figure 2(C)) and/or higher ^{56}Ni-mixing in comparison to SN 2018hna and other events. Post-maximum, the colors turn redder and are similar to SN 1987A during the transition to the radioactive decay phase (beyond ∼125 days).

It is seen that the progenitors of 1987A-like events produce higher amount of ^{56}Ni in comparison to normal SNe II as majority of them have higher ejecta masses (Taddia et al. 2016). The degree of ^{56}Ni-mixing and the net amount of ^{56}Ni synthesized helps change the rise to the maximum. A larger ^{56}Ni mass increases the time taken to rise to the bolometric peak (rise time) and brightens the peak, whereas a higher degree of ^{56}Ni-mixing decreases the rise time.

The optical (*UBVRI*) bolometric luminosity of SN 2018hna is higher than SN 1987A during the maximum and the radioactive decay phase (Figure 5(A)). The bolometric luminosity including the NIR contribution (*UBVRIJHKs*) of SN 2018hna is 16 ± 5% brighter than SN 1987A during the radioactive decay phase (∼150 days). Hence, the ^{56}Ni synthesized in SN 2018hna is 0.087 ± 0.004 $M_{\odot}$. The rise

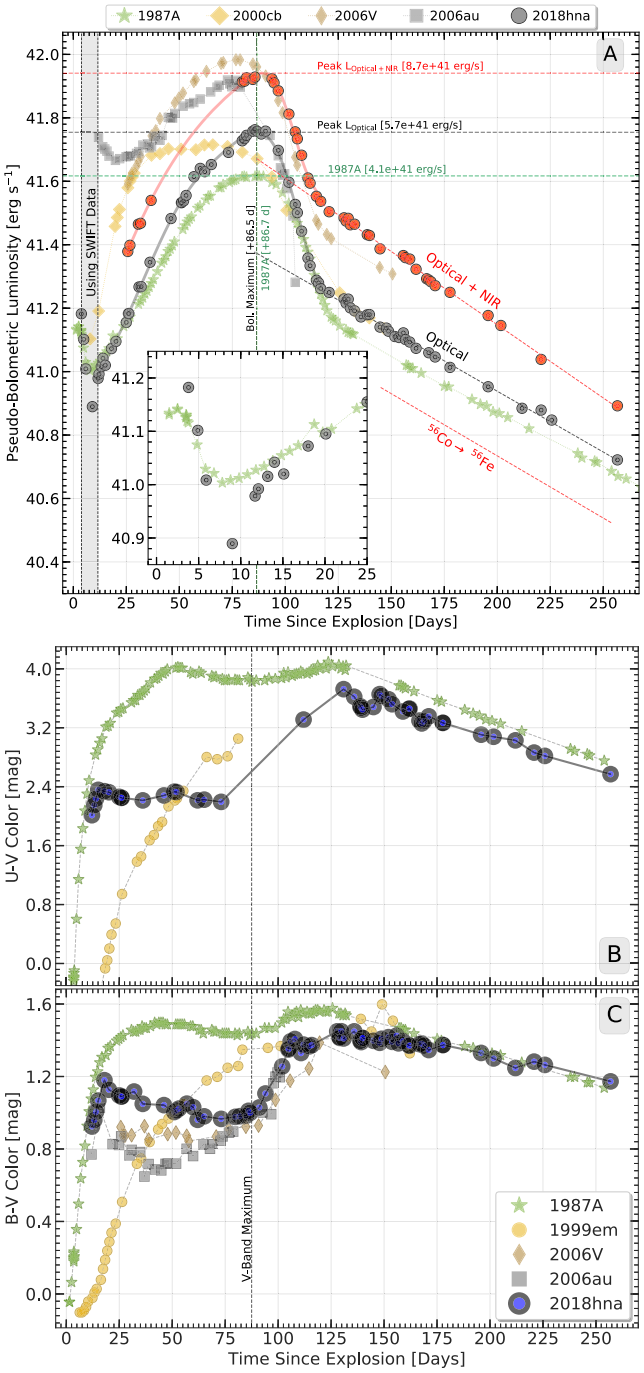

Figure 5. Panel (A): pseudo-bolometric light curve of SN 2018hna in comparison with 1987A-like events. Panels (B) and (C): *(U–V)* and *(B–V)* color evolution of SN 2018hna in comparison with 1987A-like events and SN 1999em.

to the bolometric maximum is steeper in SN 2018hna in comparison to SN 1987A and signifies a slightly lower degree of ^{56}Ni-mixing in its ejecta. The luminosity at the maximum of 1987A-like events is roughly ∼1.5 times the luminosity from the radioactive decay (Dessart & Hillier 2019); however, in the case of SN 2018hna it is more than twice (∼2.5).

Blueshifted emission lines in the nebular phase are shown to be an indicator of dust formation in the ejecta of SNe (Elmhamdi et al. 2003) as the receding component of ejecta is blocked by the newly synthesized dust (Sarangi et al. 2018). Blueshifted emission of [O I], Hα, and [Ca II] is seen during the nebular phase of SN 2018hna (see the right panel in Figure 3). The peak of these emission lines stays at almost constant velocities of ∼1200, 600, and 1100 km s^{-1}, respectively, throughout the nebular phase. These numbers are consistent with the fact that oxygen and calcium are found deeper in the ejecta than hydrogen. The first overtone of CO emission (∼2.3 μm) was detected in SN 2018hna in the near-infrared spectrum of ∼153 days (Rho et al. 2019). A similar feature was also detected in SN 1987A around ∼136 days. In all, the signatures above are an indication of dust in the ejecta of SN 2018hna.

6. Summary

A detailed analysis of the photometric and spectroscopic evolution of the SN 1987A-like supernova SN 2018hna is presented in this Letter, based on which the following are inferred:

1. Signature of shock breakout is seen in the early phase. SN 2018hna is only the second BSG event caught within a few days from shock breakout.
2. The rise to maximum is slow, similar to other 1987A-like events, with a peak *V*-band absolute magnitude of -16.35 ± 0.32 mag.
3. An explosion energy of ∼(1.7–2.9) × 10^{51}erg, a BSG progenitor with a radius ∼50 $R_{\odot}$, and mass ∼14–20 $M_{\odot}$.
4. A subsolar metallicity (∼0.3 $Z_{\odot}$) for the host galaxy UGC 07534, in coherence with the low-metallicity of other 1987A-like events.

We thank the referee for positive comments on the manuscript. We thank Masaomi Tanaka for his insightful suggestions. We thank the staff of IAO-Hanle, CREST-Hosakote, Higashi-Hiroshima Observatory, and Okayama Observatory who made these observations possible. The facilities at IAO and CREST are operated by the Indian Institute of Astrophysics (IIA), Bangalore. The 0.7 m GIT is set up by IIA and the Indian Institute of Technology, Bombay at IAO, Hanle with support from the Indo-US Science and Technology Forum (IUSSTF) and the Science and Engineering Research Board (SERB) of the Department of Science and Technology (DST), Government of India grant No. IUSSTF/PIRE Program/GROWTH/2015-16. G.C.A. and V. B. acknowledge the SERB-IUSSTF grants for the same.

D.K.S. and G.C.A. acknowledge DST/JSPS grant DST/INT/JSPS/P/281/2018. H.K. thanks the LSSTC Data Science Fellowship Program, which is funded by LSSTC, NSF Cybertraining grant #1829740, the Brinson Foundation, and the Moore Foundation. P.V.B.'s work on finding parameters of SNe is supported by the grant RSF 18-12-00522. S.B. is supported by the grant RSF 19-12-00229 in his work on developing codes modeling the radiative transfer in SNe. K.M acknowledges support by JSPS KAKENHI grant (18H05223) for the initiation of the SN follow-up program with the Seimei telescope. This research has been supported in part by the RFBR-JSPS bilateral program.

This research made use of RedPipe,[18] an assemblage of data reduction and analysis scripts written by A.S. We acknowledge Wiezmann Interactive Supernova data

[18] https://github.com/sPaMFouR/RedPipe

REPository[19] (WISeREP; Yaron & Gal-Yam 2012) and ESA *Gaia*, DPAC, and the Photometric Science Alerts Team.[20]

Facilities: HCT (HFOSC), GIT, KT (HOWPol, HONIR), ST (KOOLS-IFU), Swift (UVOT) .

Software: STELLA, Astropy (v3.1.2), SciPy (v1.3.0), Matplotlib (v3.1.0), Pandas (v0.24.2), PyRAF (v2.1.14), Seaborn (v0.9.0).

ORCID iDs

Avinash Singh https://orcid.org/0000-0003-2091-622X
G. C. Anupama https://orcid.org/0000-0003-3533-7183
Brajesh Kumar https://orcid.org/0000-0001-7225-2475
Masayuki Yamanaka https://orcid.org/0000-0001-9456-3709
Nozomu Tominaga https://orcid.org/0000-0001-8537-3153
Keiichi Maeda https://orcid.org/0000-0003-2611-7269
Varun Bhalerao https://orcid.org/0000-0002-6112-7609
Sudhanshu Barway https://orcid.org/0000-0002-3927-5402
Koji S Kawabata https://orcid.org/0000-0001-6099-9539
Mahito Sasada https://orcid.org/0000-0001-5946-9960
Takashi Nagao https://orcid.org/0000-0002-3933-7861

References

Akitaya, H., Moritani, Y., Ui, T., et al. 2014, Proc. SPIE, 9147, 91474O
Anderson, J. P., Dessart, L., Gutierrez, C. P., et al. 2014, MNRAS, 441, 671
Arnett, W. D. 1979, ApJL, 230, L37
Bellm, E. C., Kulkarni, S. R., Graham, M. J., et al. 2019, PASP, 131, 018002
Bersten, M. C., Benvenuto, O. G., Nomoto, K., et al. 2012, ApJ, 757, 31
Blinnikov, S., Lundqvist, P., Bartunov, O., Nomoto, K., & Iwamoto, K. 2000, ApJ, 532, 1132
Dessart, L., & Hillier, D. J. 2019, A&A, 622, A70
Elmhamdi, A., Danziger, I. J., Chugai, N., et al. 2003, MNRAS, 338, 939
Ensman, L., & Burrows, A. 1992, ApJ, 393, 742
Falk, S. W., & Arnett, W. D. 1977, ApJS, 33, 515
Fremling, C., Ko, H., Dugas, A., et al. 2019, ApJL, 878, L5
Gaia Collaboration, Brown, A. G. A., Vallenari, A., et al. 2018, A&A, 616, A1
Gehrels, N., Chincarini, G., Giommi, P., et al. 2004, ApJ, 611, 1005
Gezari, S., Rest, A., Huber, M. E., et al. 2010, ApJL, 720, L77
Grassberg, E. K., Imshennik, V. S., & Nadyozhin, D. K. 1971, Ap&SS, 10, 28
Hamuy, M., & Suntzeff, N. B. 1990, AJ, 99, 1146
Hanuschik, R. W., Thimm, G., & Dachs, J. 1988, MNRAS, 234, 41P
Heger, A., Fryer, C. L., Woosley, S. E., Langer, N., & Hartmann, D. H. 2003, ApJ, 591, 288
Karachentsev, I. D., Makarov, D. I., & Kaisina, E. I. 2013, AJ, 145, 101
Kawabata, K. S., Nagae, O., Chiyonobu, S., et al. 2008, Proc. SPIE, 7014, 70144L
Kelly, P. L., Rodney, S. A., Treu, T., et al. 2016, ApJL, 819, L8
Kleiser, I. K. W., Poznanski, D., Kasen, D., et al. 2011, MNRAS, 415, 372
Kumar, B., Pandey, S. B., Sahu, D. K., et al. 2013, MNRAS, 431, 308
Kumar, B., Singh, A., Srivastav, S., Sahu, D. K., & Anupama, G. C. 2018, MNRAS, 473, 3776
Matsubayashi, K., Ohta, K., Iwamuro, F., et al. 2019, arXiv:1905.05430
Mazzali, P. A., & Chugai, N. N. 1995, A&A, 303, 118
Nakar, E., & Piro, A. L. 2014, ApJ, 788, 193
Nakar, E., & Sari, R. 2010, ApJ, 725, 904
Ofek, E. O., Fox, D., Cenko, S. B., et al. 2013, ApJ, 763, 42
Pastorello, A., Baron, E., Branch, D., et al. 2005, MNRAS, 360, 950
Pastorello, A., Pumo, M. L., Navasardyan, H., et al. 2012, A&A, 537, A141
Pastorello, A., Valenti, S., Zampieri, L., et al. 2009, MNRAS, 394, 2266
Phillips, M. M., & Heathcote, S. R. 1989, PASP, 101, 137
Podsiadlowski, P. 1992, PASP, 104, 717
Pun, C. S. J., Kirshner, R. P., Sonneborn, G., et al. 1995, ApJS, 99, 223
Rho, J., Shahbandeh, M., Hsiao, E., & Davis, S. 2019, ATel, 12897, 1
Richmond, M. W., Treffers, R. R., Filippenko, A. V., et al. 1994, AJ, 107, 1022
Rodney, S. A., Strolger, L. G., Kelly, P. L., et al. 2016, ApJ, 820, 50
Roming, P. W. A., Kennedy, T. E., Mason, K. O., et al. 2005, SSRv, 120, 95
Sarangi, A., Matsuura, M., & Micelotta, E. R. 2018, SSRv, 214, 63
Schlafly, E. F., & Finkbeiner, D. P. 2011, ApJ, 737, 103
Singh, A., Srivastav, S., Kumar, B., Anupama, G. C., & Sahu, D. K. 2018, MNRAS, 480, 2475
Smartt, S. J. 2009, ARA&A, 47, 63
Smith, K. W., Williams, R. D., Young, D. R., et al. 2019, RNAAS, 3, 26
Taddia, F., Sollerman, J., Fremling, C., et al. 2016, A&A, 588, A5
Taddia, F., Stritzinger, M. D., Sollerman, J., et al. 2012, A&A, 537, A140
Takáts, K., Pignata, G., Bersten, M., et al. 2016, MNRAS, 460, 3447
Tominaga, N., Blinnikov, S., Baklanov, P., et al. 2009, ApJL, 705, L10
Tremonti, C. A., Heckman, T. M., Kauffmann, G., et al. 2004, ApJ, 613, 898
Utrobin, V. P., & Chigai, N. N. 2011, A&A, 532, A100
Yaron, O., & Gal-Yam, A. 2012, PASP, 124, 668

[19] https://wiserep.weizmann.ac.il
[20] http://gsaweb.ast.cam.ac.uk/alerts